A Finite Volume Scheme for Solving Elliptic Boundary Value Problems on Composite Grids

M.J.H. Anthonissen, B. van 't Hof, Eindhoven, and **A.A. Reusken**, Aachen

Abstract

We present a finite volume scheme for solving elliptic boundary value problems with solutions that have one or a few small regions with high activity. The scheme results from combining the local defect correction method (LDC), introduced in [11], with standard finite volume discretizations on a global coarse and on local fine uniform grids. The iterative discretization method that is obtained in this way yields a discrete approximation of the continuous solution on a composite grid.

For the LDC method in its standard form, the discrete conservation property, which is one of the main attractive features of a finite volume method, is lost for the composite grid approximation. For the modified LDC method we present here, discrete conservation holds for the composite grid solution, too.

AMS Subject Classifications: 65N22, 65N50.

Key words: Elliptic problems, finite volume methods, local defect correction, composite grids.

1 Introduction

Many boundary value problems produce solutions that have highly localized properties. In this paper we consider elliptic boundary value problems with solutions that have one or a few small regions with high activity.

We study a finite volume discretization method based on a combination of *standard finite volume discretizations on several uniform grids with different grid sizes that cover different parts of the domain.* At least one grid should cover the entire domain; the meshsize of this *global coarse grid* is chosen in agreement with the relatively smooth behavior of the solution outside the high activity regions. Apart from this global coarse grid, one or several *local grids* are used which are also uniform. Each of these local grids covers only a (small) part of the domain and contains a high activity region. The meshsizes of the local grids are chosen in agreement with the behavior of the solution in the corresponding high activity region. In this way, every part of the domain can be covered by a (locally) uniform grid with a meshsize that is in agreement with the behavior of the continuous solution in that part of the domain. This refinement strategy is known as *locally uniform grid refinement.* The solution is approximated on the *composite grid*, which is the union of the uniform subgrids. Note that such composite grids are highly structured and hence very simple data structures can be used.

In [11], Hackbusch introduced the *local defect correction method* (LDC) for approximating the continuous solution of elliptic boundary value problems on a composite grid. In this method, which is an iterative process, a basic global discretization is improved by local discretizations

defined in the subdomains. This update of the coarse grid solution is achieved by putting a defect correction term in the right hand side of the coarse grid problem. At each iteration step, the process yields a discrete approximation of the continuous solution on the composite grid. The discrete problem that is actually being solved is an implicit result of the iterative process. Therefore, the LDC method is both an iterative discretization and solution method. An analysis of the LDC technique in combination with finite difference discretizations is presented in [5–7].
In this paper, we consider the integral formulation of a two-dimensional convection-diffusion problem, and combine the LDC technique with standard finite volume discretizations of this problem on the global coarse and local fine grids. In the LDC method as in [5–7, 11], the discrete conservation property, which is one of the main attractive features of a finite volume method, does *not* hold for the composite grid approximation. Here, we present a *modified* LDC method, which is based on a special form of the defect correction term used in the right hand side of the coarse grid problem. Due to this finite volume adapted defect correction term, the *conservation property is preserved* in the discretization on the composite grid.

Attractive features of the finite volume based LDC method presented here are:

- the method yields a discretization on locally refined grids;
- a discrete conservation property holds for the discretization on the composite grid;
- the method is simple: it only uses standard finite volume discretizations on uniform (global coarse and local fine) grids.

Discretization methods on composite grids have been discussed by other authors too. McCormick presents the finite volume element (FVE) method, which is used in the fast adaptive composite grid (FAC) method (cf. [15–17]). Ewing *et al.* [3, 4] give an analysis of a finite volume based local refinement technique with composite grids. In both approaches, an *explicit* discretization scheme for the composite grid is proposed, in which special difference stars near the composite grid interfaces are used. The resulting discrete system is then solved by an iterative method (e.g. FAC) which may take advantage of the composite grid structure. This is a crucial difference with the LDC method, which combines standard discretizations on uniform grids only and does not use an a priori given composite grid discretization.

This paper is organized as follows. In Section 2, we formulate a stationary convection-diffusion problem, and discuss a standard vertex-centered finite volume technique for discretizing this problem on a uniform grid. In Section 3, we briefly recall the concept of composite grids, and derive a finite volume adapted LDC method. For the resulting composite grid discretization, we prove a discrete conservation property. In Section 4, we show results of a few numerical experiments.

2 Problem formulation and finite volume discretization on a uniform grid

We consider a stationary convection-diffusion problem in the domain $\Omega = (0,1) \times (0,1)$ with Dirichlet boundary conditions $\varphi = \psi$ on $\partial\Omega$. By $V \subset \Omega$ we denote a generic Lipschitz subdomain of Ω. The outward unit normal vector to ∂V is denoted by $\mathbf{n}$. We assume given functions $\Gamma = \Gamma(x,y) \geq \Gamma_{\min} > 0$ (diffusion coefficient), $\mathbf{v} = (v_1(x,y), v_2(x,y))^T$ (mass flux), and $s = s(x, y)$ (source term). Introducing the flux vector

$$\mathbf{f}_\varphi = (f, g)^T = \mathbf{v}\varphi - \Gamma \nabla \varphi, \tag{1}$$

the problem we consider can be represented in *integral formulation* as: determine $\varphi \in H^1(\Omega)$ with $\varphi|_{\partial\Omega} = \psi$ (in the sense of traces), such that

$$\oint_{\partial V} \mathbf{f}_\varphi \cdot \mathbf{n}\, d\gamma = \int_V s\, d\Omega, \quad \text{for all } V. \tag{2}$$

Here we used standard notation for the Sobolev space $H^1(\Omega)$. In this paper, we study a finite volume discretization technique based on a combination of finite volume discretizations on several uniform grids with different meshsizes. For the discretization of the convection-diffusion problem on the *uniform* grids, we consider a standard *vertex-centered* finite volume discretization method. The technique we present may be generalized, however, to cell-centered methods and to so-called structured boundary conforming grids (cf. [19]) or to logically rectangular grids, cf. Remarks 3 and 8.

The finite volume discretizations on the uniform grids are standard and can be found in many textbooks; the presentation, however, is adapted to the generalization to composite grids. We use a meshsize parameter $H = 1/(N+1)$, $N \in I\!N$, and grid points $(x_i, y_j) := (iH, jH)$, $(x_{i+1/2}, y_j) := ((i+1/2)H, jH)$, $(x_i, y_{j+1/2}) := (iH, (j+1/2)H)$, $i, j \in I\!N$. In a vertex-centered approach one uses a *computational grid* Ω^H defined by

$$\bar{\Omega}^H := \{(x_i, y_j)\} \cap \bar{\Omega}, \qquad \partial\bar{\Omega}^H := \bar{\Omega}^H \cap \partial\Omega, \qquad \Omega^H := \bar{\Omega}^H \setminus \partial\bar{\Omega}^H,$$

and a *control volume* V_{ij} around each grid point in Ω^H

$$V_{ij} := (x_{i-1/2}, x_{i+1/2}) \times (y_{j-1/2}, y_{j+1/2}). \tag{3}$$

The midpoints of the interfaces of these volumes form a dual grid

$$V^H := \big(\{(x_{i+1/2}, y_j)\} \cup \{(x_i, y_{j+1/2})\}\big) \cap \Omega,$$

on which we will define discrete fluxes. The spaces of grid functions on Ω^H, $\bar{\Omega}^H$, V^H are denoted by $G(\Omega^H)$, $G(\bar{\Omega}^H)$, $G(V^H)$, respectively. For grid functions we use boldface notation; for $\mathbf{F}^H \in G(\Omega^H)$, we write $\mathbf{F}^H = (F^H_{ij})_{1 \le i,j \le N}$ with $F^H_{ij} := \mathbf{F}^H(x_i, y_j)$. We use a similar notation for elements in $G(\bar{\Omega}^H)$, $G(V^H)$. We introduce, for $\mathbf{F}^H \in G(V^H)$, central difference operators ∇^H_x, ∇^H_y : $G(V^H) \to G(\Omega^H)$ by

$$(\nabla^H_x \mathbf{F}^H)_{ij} := F^H_{i+1/2,j} - F^H_{i-1/2,j}, \qquad (\nabla^H_y \mathbf{F}^H)_{ij} := F^H_{i,j+1/2} - F^H_{i,j-1/2}.$$

We define the *continuous flux* $\mathbf{F}(\varphi) \in G(V^H)$ as follows (cf. (1)):

$$F_{i+1/2,j} := \int_{y_{j-1/2}}^{y_{j+1/2}} f(x_{i+1/2}, \eta)\, d\eta, \qquad F_{i,j+1/2} := \int_{x_{i-1/2}}^{x_{i+1/2}} g(\xi, y_{j+1/2})\, d\xi. \tag{4}$$

Note that this is the continuous flux over the interfaces of the control volumes V_{ij} as in (3). Finally, we define $\mathbf{S} \in G(\Omega^H)$ by

$$S_{ij} := \int_{V_{ij}} s\, d\Omega. \tag{5}$$

Applying the conservation law in (2) with $V = V_{ij}$ yields:

$$\left(\nabla_x^H \mathbf{F}(\varphi)\right)_{ij} + \left(\nabla_y^H \mathbf{F}(\varphi)\right)_{ij} = S_{ij}. \tag{6}$$

In finite volume discretizations the continuous fluxes in (4), which depend on the continuous solution φ, are approximated using a finite difference scheme. For $\boldsymbol{\xi} \in G(\bar{\Omega}^H)$, we introduce a *discrete flux* grid function $\mathbf{F}^H(\boldsymbol{\xi}) \in G(V^H)$. Here we use a general setting and we will not be specific about the particular finite difference scheme that is used. We only assume that the difference scheme $\mathbf{F}^H(\boldsymbol{\xi})$ is local and linear in $\boldsymbol{\xi}$, i.e.,

$$F_{i+1/2,j}^H(\boldsymbol{\xi}) = \sum_{k=0,1,\, m=-1,0,1} \alpha_{i+k,j+m}\, \xi_{i+k,j+m}, \tag{7}$$

with given coefficients $\alpha_{pq} \in I\!R$. We use a similar approximation $F_{i,j+1/2}^H$. In practice, the integral in (5) is approximated by a quadrature rule. The resulting approximation of $\mathbf{S}$ is denoted by $\mathbf{S}^H$.

Example 1 If we apply the midpoint rule to approximate the integrals in (4), (5), and use central differences to approximate the fluxes at midpoints of volume faces, we obtain for $\mathbf{F}^H(\boldsymbol{\xi})$ and $\mathbf{S}^H$

$$F_{i+1/2,j}^H = f_{i+1/2,j}^H\, H, \qquad F_{i,j+1/2}^H = g_{i,j+1/2}^H\, H, \qquad S_{ij}^H = s(x_i, y_j)\, H^2,$$

where

$$\begin{aligned} f_{i+1/2,j}^H &= v_1(x_{i+1/2}, y_j)\, \frac{\xi_{ij} + \xi_{i+1,j}}{2} - \Gamma(x_{i+1/2}, y_j)\, \frac{\xi_{i+1,j} - \xi_{ij}}{H}, \\ g_{i,j+1/2}^H &= v_2(x_i, y_{j+1/2})\, \frac{\xi_{ij} + \xi_{i,j+1}}{2} - \Gamma(x_i, y_{j+1/2})\, \frac{\xi_{i,j+1} - \xi_{ij}}{H}. \end{aligned}$$

In the above, $\boldsymbol{\xi} \in G(\bar{\Omega}^H)$, $\mathbf{F}^H(\boldsymbol{\xi}) \in G(V^H)$, and $\mathbf{S}^H \in G(\Omega^H)$. $\square$

In (6), we replace the continuous fluxes $\mathbf{F}$ by approximate fluxes $\mathbf{F}^H$ as in (7) and S_{ij} by S_{ij}^H. We then obtain a finite volume discretization which can be represented as:

$$\begin{cases} \text{find } \boldsymbol{\varphi}^H \in G(\bar{\Omega}^H) \text{ such that:} \\ \nabla_x^H \mathbf{F}^H(\boldsymbol{\varphi}^H) + \nabla_y^H \mathbf{F}^H(\boldsymbol{\varphi}^H) = \mathbf{S}^H, \\ \boldsymbol{\varphi}^H = \psi \text{ on } \partial\bar{\Omega}^H. \end{cases} \tag{8}$$

This discretization yields N^2 equations for the N^2 unknown values of $\boldsymbol{\varphi}^H$ on Ω^H.

3 An iterative finite volume discretization on composite grids

In this section, we will present a finite volume method for approximating the continuous solution φ on a *composite grid*. In Section 3.1, we explain how a composite grid is formed by combining two or more uniform grids with different meshsizes. In Section 3.2, we adapt the general Local Defect Correction (LDC) method from [11] to a finite volume setting. The LDC method is an iterative method, hence we obtain an iterative finite volume discretization method. In Section 3.3, we derive some properties of the method. In particular it is shown that a conservation property holds on the composite grid.

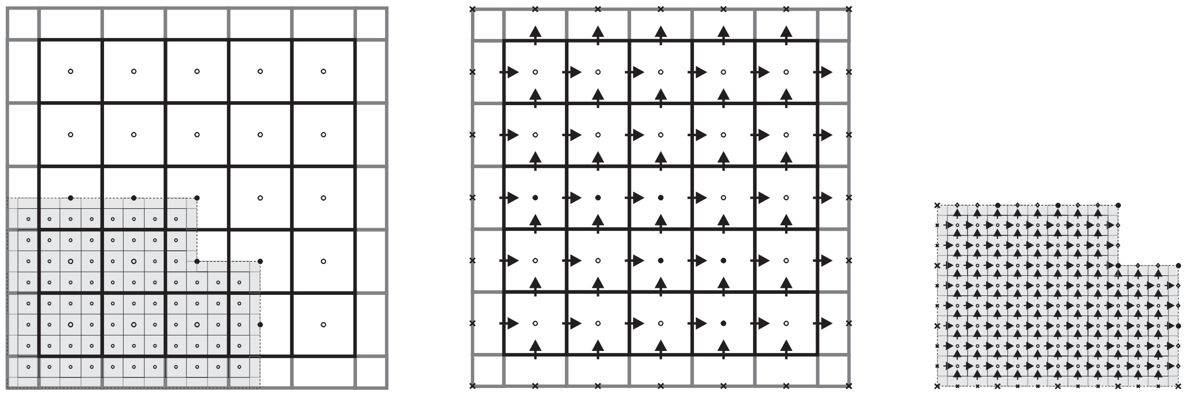

Figure 1: A composite, global coarse and local fine grid; $H = 1/6$, $N = 5$, and the refinement factor σ equals 3. Grid points, control volumes, and fluxes are denoted by little circles, large squares, and arrows, respectively. The shaded region is Ω_l; the points of Γ^H are marked by filled circles.

3.1 Composite grid

In this section we recall the concept of composite grids and introduce some notation. Composite grids can be found in e.g. [1–3, 8–10, 15]. The grids we consider result from a uniform basis grid with meshsize H, cf. Section 2, that is extended with a region of *locally uniform refinement* Ω_l, which is such that it contains the part(s) of Ω in which relatively high resolution is needed. In Section 4, an example of an interface problem is given, where it is a priori clear that in a (small) part of the domain Ω a much higher resolution is required than in the remaining part. Further examples can be found in [5, 7, 11].

The uniform basis grid, denoted by Ω^H, is called the *global coarse grid*. We assume that $\Omega_l \subseteq \Omega$ is chosen such that

$$(x_i, y_j) \in \Omega^H \cap \Omega_l \iff W_{ij} \subset \Omega_l \tag{9}$$

holds with

$$W_{ij} := (x_{i-1}, x_{i+1}) \times (y_{j-1}, y_{j+1}). \tag{10}$$

Note that $V_{ij} \subset W_{ij}$, so that $W_{ij} \subset \Omega_l$ implies $V_{ij} \subset \Omega_l$. Also, Ω_l is not a union of control volumes V_{ij}. In Ω_l we apply, as in Ω, a vertex-centered finite volume method, i.e., we first introduce a uniform computational grid with meshsize $h < H$. This grid, which is denoted by Ω_l^h, is called the *local fine grid*. To make sure that grid points in $\Omega_l^H := \Omega^H \cap \Omega_l$ are grid points of Ω_l^h, and that boundaries of control volumes in the local fine grid coincide with boundaries of control volumes in the global coarse grid, we *assume the refinement factor*

$$\sigma := H/h$$

to be an odd integer. We emphasize that a refinement factor $\sigma \gg 1$ is allowed, i.e., we can use a global coarse grid and a local fine grid with different resolution properties. In Figure 1, an example of a composite grid is shown (cf. also Section 4).
The interface between the global coarse grid and the local fine grid will be denoted by $\Gamma := \partial\Omega_l \setminus \partial\Omega$. We will call the set of coarse grid points on this boundary Γ^H, so $\Gamma^H := \Gamma \cap \Omega^H$. The composite grid is denoted by $\Omega^{H,h} := \Omega^H \cup \Omega_l^h$, $\bar{\Omega}^{H,h} := \bar{\Omega}^H \cup \Omega_l^h$.

3.2 A Local Defect Correction finite volume discretization

Basically, the LDC iteration in [11] consists of the following steps:

1. Solve a *global coarse* grid problem with given right hand side.
2. Solve a *local fine* grid problem with artificial boundary conditions on the interface Γ.
3. Compute a *defect correction* term for the right hand side of the coarse grid problem, and go to 1.

Below, we discuss these three steps, resulting in the algorithm in (23)–(25). For adapting the general LDC method from [11] to a finite volume setting, the key point is a defect correction (Step 3) which is based on discretization error estimates for the numerical *fluxes*.

Global coarse grid problem

We compute an initial approximation $\boldsymbol{\varphi}^H$ on the global coarse grid using the standard finite volume discretization of Section 2, i.e., $\boldsymbol{\varphi}^H$ is the solution of the discrete problem (8).

Local fine grid problem

We formulate a boundary value problem on the local domain Ω_l, using the coarse grid approximation to define *artificial Dirichlet boundary conditions* on the interface Γ. To determine the artificial boundary conditions, we use an interpolation operator $p : \Gamma^H \to \Gamma$; obvious choices for p are the linear and the quadratic interpolation operator. Due to the fact that Ω_l is, by construction, a union of sets W_{ij}, a linear interpolation $p : \Gamma^H \to \Gamma$ can be defined in a straightforward manner. If a point x on a vertical (horizontal) part of Γ has (at least) three neighboring points in Γ^H which lie on a vertical (horizontal) line, a quadratic interpolation at x can be defined in a natural way. At $\partial\Omega_l \cap \partial\Omega$ we use the given Dirichlet boundary conditions.

We are thus led to an analogon of problem (2) on the subdomain Ω_l with artificial boundary conditions on the interface Γ. We discretize this problem on the uniform local grid Ω_l^h using the method described in Section 2. We use a notation in which local fine grid quantities are denoted by a subscript l and a superscript h, e.g.: Ω_l^h (computational grid on Ω_l), V_l^h (dual grid on Ω_l), $G(V_l^h)$ (grid functions on V_l^h) and, for $\boldsymbol{\xi} \in G(\bar{\Omega}_l^h)$, $\mathbf{F}_l^h(\boldsymbol{\xi}) \in G(V_l^h)$ (discrete flux on V_l^h). These quantities related to Ω_l are defined in exactly the same way as their analogons in Section 2 which are related to Ω.

Using this notation the *discrete local fine grid* problem can be formulated as:

$$\begin{cases} \text{find } \boldsymbol{\varphi}_l^h \in G(\bar{\Omega}_l^h) \text{ such that:} \\ \nabla_x^h \mathbf{F}_l^h(\boldsymbol{\varphi}_l^h) + \nabla_y^h \mathbf{F}_l^h(\boldsymbol{\varphi}_l^h) = \mathbf{S}_l^h, \\ \boldsymbol{\varphi}_l^h = \psi \text{ on } \partial\bar{\Omega}_l^h \cap \partial\Omega, \qquad \boldsymbol{\varphi}_l^h = p(\boldsymbol{\varphi}^H|_{\Gamma^H}) \text{ on } \partial\bar{\Omega}_l^h \cap \Gamma. \end{cases} \tag{11}$$

The discrete solutions $\boldsymbol{\varphi}^H$ and $\boldsymbol{\varphi}_l^h$ yield an approximation of φ at all points of the composite grid. We denote this *composite grid approximation* by $\boldsymbol{\varphi}^{H,h}$, and take the newest values in grid points belonging to both the coarse grid and the fine grid, viz.

$$\boldsymbol{\varphi}^{H,h} := \begin{cases} \boldsymbol{\varphi}_l^h, & \text{on } \Omega_l^h, \\ \boldsymbol{\varphi}^H, & \text{on } \bar{\Omega}^H \setminus \Omega_l^H. \end{cases} \tag{12}$$

Defect correction

We now derive the third step in the algorithm, in which we use the (more accurate) approximation found on the local fine grid to compute a correction for the right hand side of the global coarse grid problem.
Substitution of the continuous solution φ in (8) yields a defect

$$\mathbf{d}^H := \nabla_x^H \mathbf{F}^H(\varphi|_{\bar{\Omega}^H}) + \nabla_y^H \mathbf{F}^H(\varphi|_{\bar{\Omega}^H}) - \mathbf{S}^H. \tag{13}$$

Combination of (6) and (13) yields:

$$\mathbf{d}^H = \nabla_x^H(\mathbf{F}^H(\varphi|_{\bar{\Omega}^H}) - \mathbf{F}(\varphi)) + \nabla_y^H(\mathbf{F}^H(\varphi|_{\bar{\Omega}^H}) - \mathbf{F}(\varphi)) - (\mathbf{S}^H - \mathbf{S}). \tag{14}$$

This expression for the coarse grid defect is used to derive an approximation for $\mathbf{d}^H$ by estimating the flux discretization error $\mathbf{F}^H(\varphi|_{\bar{\Omega}^H}) - \mathbf{F}(\varphi)$ and the source term discretization error $\mathbf{S}^H - \mathbf{S}$.

After solving the global coarse and local fine grid problems, the following approximations are available for an arbitrary horizontal flux $F_{i+1/2,j}(\varphi)$:

1. the coarse grid approximation of the flux, $F^H_{i+1/2,j}(\boldsymbol{\varphi}^H)$;
2. a coarse grid approximation of the flux based on the most recently calculated approximation for φ, i.e., $F^H_{i+1/2,j}(\boldsymbol{\varphi}^{H,h}|_{\bar{\Omega}^H})$;
3. a sum of fine grid approximations of fluxes,

$$F^{\text{sum}}_{l,i+1/2,j}(\boldsymbol{\varphi}_l^h) := \sum_{k=-(\sigma-1)/2}^{(\sigma-1)/2} F^h_{l,i+1/2,j+k}(\boldsymbol{\varphi}_l^h). \tag{15}$$

   This third approximation only exists, if $(x_{i+1/2}, y_j) \in \Omega_l$, i.e., if the cell face $(x_{i+1/2}, y_{j-1/2}) \times (x_{i+1/2}, y_{j+1/2})$ lies in the area of refinement.

Note that both in the second and third approximation, we use the solution $\boldsymbol{\varphi}_l^h$ of the discrete local fine grid problem (11). In the second approximation, however, only a coarse grid flux discretization F^H is used, whereas in the third approximation, a fine grid flux discretization F_l^h is used, too. These three approximations are considered to be listed in order of increasing accuracy. Because similar approximations are available for the other fluxes, $F_{i-1/2,j}(\varphi)$, $F_{i,j+1/2}(\varphi)$, $F_{i,j-1/2}(\varphi)$, too, we can define a coarse grid flux vector which uses information from the local fine grid solution: $\mathbf{F}^{\text{best}}(\boldsymbol{\varphi}^{H,h}) \in G(V^H)$ is defined by:

$$\mathbf{F}^{\text{best}}(\boldsymbol{\varphi}^{H,h}) := \begin{cases} \mathbf{F}_l^{\text{sum}}(\boldsymbol{\varphi}_l^h), & \text{on } V^H \cap \Omega_l \text{ (as in (15))}, \\ \mathbf{F}^H(\boldsymbol{\varphi}^{H,h}|_{\bar{\Omega}^H}), & \text{elsewhere}. \end{cases} \tag{16}$$

We use this flux vector to give the following flux discretization error estimate

$$\mathbf{F}^H(\varphi|_{\bar{\Omega}^H}) - \mathbf{F}(\varphi) \approx \mathbf{F}^H(\boldsymbol{\varphi}^{H,h}|_{\bar{\Omega}^H}) - \mathbf{F}^{\text{best}}(\boldsymbol{\varphi}^{H,h}) =: \mathbf{d}_F^H(\boldsymbol{\varphi}^{H,h}). \tag{17}$$

Analogously, we have the following approximations for an arbitrary source term S_{ij}:

1. the coarse grid approximation of the source term, S^H_{ij};

2. a sum of fine grid approximations of source terms,

$$\mathbf{S}_l^{\text{sum}}(x_i, y_j) := \sum_{k=-(\sigma-1)/2}^{(\sigma-1)/2} \sum_{m=-(\sigma-1)/2}^{(\sigma-1)/2} \mathbf{S}_l^h(x_i + kh, y_j + mh). \tag{18}$$

This second approximation only exists, if $(x_i, y_j) \in \Omega_l$, i.e., if the control volume V_{ij} lies in the area of refinement.

Again, the last approximation is considered to be most accurate, and we define $\mathbf{S}^{\text{best}} \in G(\Omega^H)$ by

$$\mathbf{S}^{\text{best}} := \begin{cases} \mathbf{S}_l^{\text{sum}}, & \text{on } \Omega_l^H \text{ (as in (18))}, \\ \mathbf{S}^H, & \text{elsewhere.} \end{cases} \tag{19}$$

We use this source term vector to give the following source term discretization error estimate

$$\mathbf{S}^H - \mathbf{S} \approx \mathbf{S}^H - \mathbf{S}^{\text{best}} =: \mathbf{d}_S^H. \tag{20}$$

Using (17) and (20) to estimate $\mathbf{d}^H$ in (14), we propose

$$\nabla_x^H \, \mathbf{d}_F^H(\boldsymbol{\varphi}^{H,h}) + \nabla_y^H \, \mathbf{d}_F^H(\boldsymbol{\varphi}^{H,h}) - \mathbf{d}_S^H \tag{21}$$

as a defect correction term in the right hand side of the coarse grid problem. Hence, we introduce the following notation for $\boldsymbol{\varphi}^{H,h} \in G(\bar{\Omega}^{H,h})$:

$$\mathbf{S}^H(\boldsymbol{\varphi}^{H,h}) := \mathbf{S}^H + \nabla_x^H \, \mathbf{d}_F^H(\boldsymbol{\varphi}^{H,h}) + \nabla_y^H \, \mathbf{d}_F^H(\boldsymbol{\varphi}^{H,h}) - \mathbf{d}_S^H. \tag{22}$$

Formulation of the LDC algorithm

Using the updated right hand side (22), we can repeat the procedure described above, i.e., solve a coarse grid problem, define artificial boundary conditions on Γ, solve a local fine grid problem, etc. This results in the following Local Defect Correction iterative method.

LDC algorithm

Initialization

Solve the basic coarse grid problem (8) for $\boldsymbol{\varphi}_0^H \in G(\bar{\Omega}^H)$.
Solve the local fine grid problem (11) for $\boldsymbol{\varphi}_{l,0}^h \in G(\bar{\Omega}_l^h)$.
Define the composite grid approximation $\boldsymbol{\varphi}_0^{H,h} \in G(\bar{\Omega}^{H,h})$ as in (12).

Iteration, $k = 1, 2, \ldots$

Compute an updated right hand side $\mathbf{S}^H(\boldsymbol{\varphi}_{k-1}^{H,h})$ as in (22).
Solve the global coarse grid problem

$$\begin{cases} \text{find } \boldsymbol{\varphi}_k^H \in G(\bar{\Omega}^H) \text{ such that:} \\ \nabla_x^H \, \mathbf{F}^H(\boldsymbol{\varphi}_k^H) + \nabla_y^H \, \mathbf{F}^H(\boldsymbol{\varphi}_k^H) = \mathbf{S}^H(\boldsymbol{\varphi}_{k-1}^{H,h}), \\ \boldsymbol{\varphi}_k^H = \psi \text{ on } \partial\bar{\Omega}^H. \end{cases} \tag{23}$$

Solve the local fine grid problem

$$\left\{\begin{array}{l}\text{find } \boldsymbol{\varphi}_{l,k}^h \in G(\bar{\Omega}_l^h) \text{ such that:} \\ \nabla_x^h \mathbf{F}_l^h(\boldsymbol{\varphi}_{l,k}^h) + \nabla_y^h \mathbf{F}_l^h(\boldsymbol{\varphi}_{l,k}^h) = \mathbf{S}_l^h, \\ \boldsymbol{\varphi}_{l,k}^h = \psi \text{ on } \partial\bar{\Omega}_l^h \cap \partial\Omega, \qquad \boldsymbol{\varphi}_{l,k}^h = p(\boldsymbol{\varphi}_k^H|_{\Gamma^H}) \text{ on } \partial\bar{\Omega}_l^h \cap \Gamma.\end{array}\right. \tag{24}$$

Define the composite grid approximation

$$\boldsymbol{\varphi}_k^{H,h} := \left\{\begin{array}{ll}\boldsymbol{\varphi}_{l,k}^h, & \text{on } \Omega_l^h, \\ \boldsymbol{\varphi}_k^H, & \text{on } \bar{\Omega}^H \setminus \Omega_l^H.\end{array}\right. \tag{25}$$

This is the LDC method as presented in [11], but now adapted to a setting with finite volume discretization. In particular, the form of the updated right hand side $\mathbf{S}^H(\boldsymbol{\varphi}_{k-1}^{H,h})$ is new. Here, the correction term is chosen such that in the limit ($k \to \infty$) the resulting composite grid discretization is still conservative; this is discussed in Section 3.3.

The computation of $\mathbf{S}^H(\boldsymbol{\varphi}_{k-1}^{H,h})$ can be simplified using the results in the following lemma.

Lemma 2 *For $\mathbf{S}^H(\boldsymbol{\varphi}_{k-1}^{H,h})$ as used in (23), we have, with $\Omega_c^H = \Omega^H \setminus (\Omega_l^H \cup \Gamma^H)$:*

$$S_{ij}^H(\boldsymbol{\varphi}_{k-1}^{H,h}) = \left\{\begin{array}{ll}\left(\nabla_x^H \mathbf{F}^H(\boldsymbol{\varphi}_{k-1}^{H,h}|_{\bar{\Omega}^H}) + \nabla_y^H \mathbf{F}^H(\boldsymbol{\varphi}_{k-1}^{H,h}|_{\bar{\Omega}^H})\right)_{ij}, & \textit{for } (x_i, y_j) \in \Omega_l^H, \\ S_{ij}^H, & \textit{for } (x_i, y_j) \in \Omega_c^H.\end{array}\right. \tag{26}$$

Proof Consider a grid point $(x_i, y_j) \in \Omega_l^H$. Adding the fine grid equations in (24) for all fine grid points in the coarse grid control volume V_{ij}, we find the following conservation property over this control volume:

$$\left(\nabla_x^H \mathbf{F}_l^{\mathrm{sum}}(\boldsymbol{\varphi}_{l,k-1}^h) + \nabla_y^H \mathbf{F}_l^{\mathrm{sum}}(\boldsymbol{\varphi}_{l,k-1}^h)\right)_{ij} = \mathbf{S}_l^{\mathrm{sum}}(x_i, y_j).$$

Using the notation in (16), (17), and (20) we now have for $(x_i, y_j) \in \Omega_l^H$:

$$\begin{aligned}\left(\mathbf{S}^H(\boldsymbol{\varphi}_{k-1}^{H,h})\right)_{ij} &= S_{ij}^H + \left(\nabla_x^H \mathbf{d}_F^H(\boldsymbol{\varphi}_{k-1}^{H,h}) + \nabla_y^H \mathbf{d}_F^H(\boldsymbol{\varphi}_{k-1}^{H,h})\right)_{ij} - \left(S_{ij}^H - \mathbf{S}_l^{\mathrm{sum}}(x_i, y_j)\right) \\ &= \left(\nabla_x^H \mathbf{F}^H(\boldsymbol{\varphi}_{k-1}^{H,h}|_{\bar{\Omega}^H}) + \nabla_y^H \mathbf{F}^H(\boldsymbol{\varphi}_{k-1}^{H,h}|_{\bar{\Omega}^H})\right)_{ij} + \\ &\qquad \mathbf{S}_l^{\mathrm{sum}}(x_i, y_j) - \left(\nabla_x^H \mathbf{F}_l^{\mathrm{sum}}(\boldsymbol{\varphi}_{l,k-1}^h) + \nabla_y^H \mathbf{F}_l^{\mathrm{sum}}(\boldsymbol{\varphi}_{l,k-1}^h)\right)_{ij} \\ &= \left(\nabla_x^H \mathbf{F}^H(\boldsymbol{\varphi}_{k-1}^{H,h}|_{\bar{\Omega}^H}) + \nabla_y^H \mathbf{F}^H(\boldsymbol{\varphi}_{k-1}^{H,h}|_{\bar{\Omega}^H})\right)_{ij},\end{aligned}$$

which proves the first part of (26).
From the definitions in (16) and (17), we obtain that $\mathbf{d}_F^H(\boldsymbol{\varphi}_{k-1}^{H,h})$ equals zero on $V^H \cap (\Omega \setminus \Omega_l)$, and hence the difference operators ∇_x^H and ∇_y^H applied to this grid function yield zero on Ω_c^H. This gives the second part of (26). □

Note that in (26) we have formulas for $\mathbf{S}^H(\boldsymbol{\varphi}_{k-1}^{H,h})$ for $(x_i, y_j) \in \Omega_l^H \cup \Omega_c^H = \Omega^H \setminus \Gamma^H$ in which the sum of fine grid fluxes $\mathbf{F}_l^{\mathrm{sum}}(\boldsymbol{\varphi}_{l,k-1}^h)$ is not needed. Such sums of fine grid fluxes have to be computed on faces of control volumes V_{ij} with $(x_i, y_j) \in \Gamma^H$ only. Also note that the term $\mathbf{S}_l^{\mathrm{sum}}$ can be avoided in the computation of $\mathbf{S}^H(\boldsymbol{\varphi}_{k-1}^{H,h})$.

Remark 3 The method presented in this section has a straightforward generalization to logically rectangular grids. Also, for the method to be applicable to three-dimensional problems, only minor modifications are needed. □

3.3 Properties of the LDC method

The LDC algorithm that is described in Section 3.2 is an iterative process, which implicitly gives a discretization of the convection-diffusion problem on a composite grid. In this section, we discuss a few properties of this discretization. Throughout this section, we will assume that the LDC iteration converges. Numerical experiments (cf. Section 4) and theoretical results in [5, 6, 11] support this assumption. A sufficient condition for the iterative process to be convergent is

$$\boldsymbol{\varphi}_k^H \to \boldsymbol{\varphi}_*^H \qquad (k \to \infty), \tag{27}$$

because this implies $\boldsymbol{\varphi}_k^H|_{\Gamma^H} \to \boldsymbol{\varphi}_*^H|_{\Gamma^H}$ $(k \to \infty)$, and therefore $\boldsymbol{\varphi}_{l,k}^h \to \boldsymbol{\varphi}_{l,*}^h$ $(k \to \infty)$. From these two limit solutions $\boldsymbol{\varphi}_*^H \in G(\bar{\Omega}^H)$ and $\boldsymbol{\varphi}_{l,*}^h \in G(\bar{\Omega}_l^h)$, we define a composite grid approximation $\boldsymbol{\varphi}_*^{H,h} \in G(\bar{\Omega}^{H,h})$ as in (25). In Lemma 4 below, it is shown that the coarse grid solution $\boldsymbol{\varphi}_*^H$ and the local fine grid solution $\boldsymbol{\varphi}_{l,*}^h$ coincide in Ω_l^H.

Lemma 4 *Assume that the local coarse grid homogeneous system*

$$\begin{cases} \nabla_x^H \mathbf{F}^H(\mathbf{v}) + \nabla_y^H \mathbf{F}^H(\mathbf{v}) = 0 \ \textit{on} \ \Omega_l^H, \\ \mathbf{v} = 0 \ \textit{on} \ \partial\bar{\Omega}_l^H \end{cases} \tag{28}$$

has only the zero solution in $G(\bar{\Omega}_l^H)$. Then the limit solution $(\boldsymbol{\varphi}_*^H, \boldsymbol{\varphi}_{l,*}^h)$ of the LDC iteration satisfies

$$\boldsymbol{\varphi}_*^H|_{\Omega_l^H} = \boldsymbol{\varphi}_{l,*}^h|_{\Omega_l^H}. \tag{29}$$

Proof From (23) and (26), we obtain, for $(x_i, y_j) \in \Omega_l^H$,

$$\left(\nabla_x^H \mathbf{F}^H(\boldsymbol{\varphi}_*^H) + \nabla_y^H \mathbf{F}^H(\boldsymbol{\varphi}_*^H)\right)_{ij} = \left(\nabla_x^H \mathbf{F}^H(\boldsymbol{\varphi}_*^{H,h}|_{\bar{\Omega}^H}) + \nabla_y^H \mathbf{F}^H(\boldsymbol{\varphi}_*^{H,h}|_{\bar{\Omega}^H})\right)_{ij}.$$

Note that $\boldsymbol{\varphi}_*^{H,h}(x_i, y_j) = \boldsymbol{\varphi}_*^H(x_i, y_j)$ for $(x_i, y_j) \in \Gamma^H$ and $\boldsymbol{\varphi}_*^{H,h}(x_i, y_j) = \boldsymbol{\varphi}_{l,*}^h(x_i, y_j)$ for $(x_i, y_j) \in \Omega_l^H$. Hence, $\mathbf{v} := \boldsymbol{\varphi}_*^H - \boldsymbol{\varphi}_*^{H,h}|_{\bar{\Omega}_l^H} \in G(\bar{\Omega}_l^H)$ satisfies the system (28). From the assumption it follows that this system only has the zero solution, hence $\mathbf{v} = 0$ on Ω_l^H, which is equivalent to (29). □

We will now discuss the conservation property which holds for the limit solution $\boldsymbol{\varphi}_*^{H,h}$ on the composite grid. Summation of the conservation laws for individual control volumes V_{ij}, cf. (6), leads to a conservation law on the union of these control volumes. This holds, because fluxes over internal faces cancel. Consider, e.g., control volumes V_{ij}, $V_{i+1,j}$ with $(x_i, y_j) \in \Omega^H$, $(x_{i+1}, y_j) \in \Omega^H$. We have

$$\oint_{\partial V_{ij}} \mathbf{f}_\varphi \cdot \mathbf{n}\, d\gamma + \oint_{\partial V_{i+1,j}} \mathbf{f}_\varphi \cdot \mathbf{n}\, d\gamma = \oint_{\partial (V_{ij} \cup V_{i+1,j})} \mathbf{f}_\varphi \cdot \mathbf{n}\, d\gamma, \tag{30}$$

which implies, that summation of the conservation laws on V_{ij} and $V_{i+1,j}$ leads to (2) with $V = V_{ij} \cup V_{i+1,j}$. The finite volume discretization on a uniform grid as described in Section 2 satisfies the discrete equivalent of (30) as is easily seen by adding the discrete conservation laws in (8). Therefore, discrete conservation holds for any subdomain of Ω which can be covered with control volumes V_{ij}. A similar result holds for the limit solution $\boldsymbol{\varphi}_*^{H,h}$ on the composite grid, as is shown in the following theorem.

Theorem 5 *Under the assumption of Lemma 4, the limit solution $\boldsymbol{\varphi}_*^{H,h} \in G(\bar{\Omega}^{H,h})$ satisfies the following system of discrete conservation laws:*

$$\nabla_x^H \mathbf{F}^{best}(\boldsymbol{\varphi}_*^{H,h}) + \nabla_y^H \mathbf{F}^{best}(\boldsymbol{\varphi}_*^{H,h}) = \mathbf{S}^{best}, \tag{31}$$

with $\mathbf{F}^{best}(\boldsymbol{\varphi}_*^{H,h})$ defined as in (16) and $\mathbf{S}^{best}$ defined as in (19).

Proof Using (22) and (23), we find

$$\begin{aligned} &\nabla_x^H \mathbf{F}^H(\boldsymbol{\varphi}_*^H) + \nabla_y^H \mathbf{F}^H(\boldsymbol{\varphi}_*^H) \\ &\qquad = \mathbf{S}^H(\boldsymbol{\varphi}_*^{H,h}) = \mathbf{S}^H + \nabla_x^H \mathbf{d}_F^H(\boldsymbol{\varphi}_*^{H,h}) + \nabla_y^H \mathbf{d}_F^H(\boldsymbol{\varphi}_*^{H,h}) - \mathbf{d}_S^H. \end{aligned} \tag{32}$$

For $\mathbf{d}_F^H(\boldsymbol{\varphi}_*^{H,h})$, we have, using (17) and Lemma 4,

$$\mathbf{d}_F^H(\boldsymbol{\varphi}_*^{H,h}) = \mathbf{F}^H(\boldsymbol{\varphi}_*^{H,h}|_{\bar{\Omega}^H}) - \mathbf{F}^{\mathrm{best}}(\boldsymbol{\varphi}_*^{H,h}) = \mathbf{F}^H(\boldsymbol{\varphi}_*^H) - \mathbf{F}^{\mathrm{best}}(\boldsymbol{\varphi}_*^{H,h}). \tag{33}$$

Substitution of (33) in (32) yields

$$\nabla_x^H \mathbf{F}^{\mathrm{best}}(\boldsymbol{\varphi}_*^{H,h}) + \nabla_y^H \mathbf{F}^{\mathrm{best}}(\boldsymbol{\varphi}_*^{H,h}) = \mathbf{S}^H - \mathbf{d}_S^H = \mathbf{S}^{\mathrm{best}},$$

which proves the theorem. □

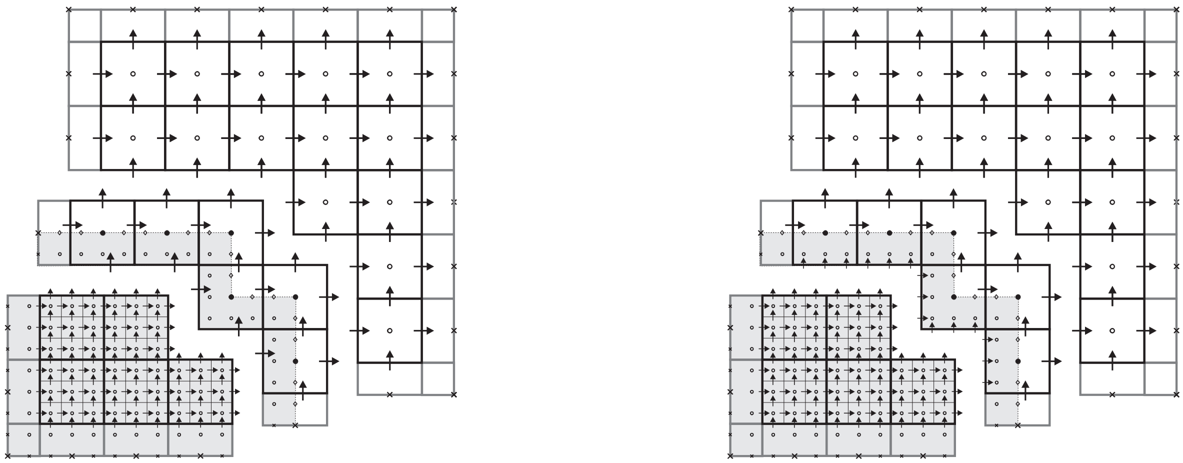

Figure 2: The discretization on the composite grid given by the LDC algorithm with the standard choice for the correction term (left figure) and with the finite volume adapted correction term (right figure).

Using Theorem 5, it is easily verified, that the discretization given by the LDC algorithm as described in Section 3.2 satisfies a discrete equivalent of (30), too. Therefore, discrete conservation holds for any subdomain of Ω which can be covered with control volumes V_{ij}.

Remark 6 For $(x_i, y_j) \in \Omega_l^H$, the conservation laws in (31) reduce to

$$\left(\nabla_x^H \mathbf{F}_l^{\text{sum}}(\boldsymbol{\varphi}_{l,*}^h) + \nabla_y^H \mathbf{F}_l^{\text{sum}}(\boldsymbol{\varphi}_{l,*}^h)\right)_{ij} = \mathbf{S}_l^{\text{sum}}(x_i, y_j). \tag{34}$$

This is the same conservation property one would obtain by adding the conservation laws that hold on the σ^2 fine grid control volumes that partition V_{ij}, cf. (24).
For $(x_i, y_j) \in \Omega^H \setminus (\Omega_l^H \cup \Gamma^H)$, the components of (31) reduce to

$$\left(\nabla_x^H \mathbf{F}^H(\boldsymbol{\varphi}_*^H) + \nabla_y^H \mathbf{F}^H(\boldsymbol{\varphi}_*^H)\right)_{ij} = \mathbf{S}^H(x_i, y_j),$$

which corresponds to the conservation laws of the finite volume discretization on the global coarse grid, cf. (8).
For $(x_i, y_j) \in \Gamma^H$, the limit discretization of the finite volume adapted LDC algorithm is such, that the discrete influx into V_{ij} out of a control volume V_{km}, $(x_k, y_m) \in \Omega_l^H$, matches the total discrete outflux from V_{km} into V_{ij}. This is illustrated in the right part of Figure 2.
If we would use the standard choice for the correction term in the LDC algorithm, the limit discretization would be the same on all control volumes V_{ij} with $(x_i, y_j) \in \Omega_l^H \cup \Omega_c^H = \Omega^H \setminus \Gamma^H$. The discretization would be different, however, on control volumes V_{ij} with $(x_i, y_j) \in \Gamma^H$; these volumes would be treated in the same way as volumes V_{ij} with $(x_i, y_j) \in \Omega_c^H$.
The difference between the discretizations given by the two LDC algorithms is clearified in Figure 2; its consequences are demonstrated by a numerical experiment in Section 4.2. $\square$

Remark 7 The system of discrete conservation laws in Theorem 5 holds for the fully converged composite grid solution $\boldsymbol{\varphi}_*^{H,h}$. However, in practice, often one or two LDC iterations

Figure 3: One-dimensional composite, global coarse and local fine grids on $(0,1)$ when a cell-centered method is used on the global coarse grid, and when the refinement factor σ is odd (left figure) and even (right figure).

will suffice to obtain a satisfactory approximation of φ on $\Omega^{H,h}$ due to the high rate of convergence of the method. Typically, one has an error reduction by a factor 10 up to 1000 in each iteration step (cf. the results in Section 4 and in [6, 11]). □

Remark 8 In Section 3.2, a vertex-centered finite volume method has been used for both the discretization on the global coarse grid and on the local fine grid.
If we would use a cell-centered method on the global coarse grid, we can cover all of Ω with control volumes, which yields global discrete conservation. This approach has been followed in the examples of Section 4. Note that, as a consequence, boundary conditions for the local fine grid problem have to be treated as in a vertex-centered method (the artificial boundary conditions) or as in a cell-centered method (the natural boundary conditions). This is illustrated in the left part of Figure 3.
It is also possible to apply a cell-centered finite volume method in Ω_l by choosing the refinement factor $\sigma = H/h$ to be an *even* integer. See the right part of Figure 3. As before, a refined coarse grid control volume is the union of fine grid control volumes, so that we can define a source term discretization error estimate in a straightforward way. However, the points in $\Omega_l^H := \Omega^H \cap \Omega_l$ are no longer grid points of Ω_l^h, so that we need to introduce a restriction $R : G(\Omega_l^h) \to G(\Omega_l^H)$ to define flux term discretization error estimates. □

4 Numerical experiments

In this section, we consider two simple numerical experiments: an interface problem in the unit square and a one-dimensional convection-diffusion problem. It should be noted, that the technique presented in Section 3 is capable of computing phenomena in more complicated geometries than treated here. The experiments have deliberately been kept simple though, while still showing the main features of the (modified) LDC algorithm. These features are:

- the method yields a discretization on a locally refined grid with an error of the same order of magnitude as a discretization on a globally refined grid (Section 4.1);
- a discrete conservation property holds on the composite grid (Section 4.2).

4.1 A two-dimensional interface problem

We consider a two-dimensional interface problem. We choose the mass flux $\mathbf{v}$ equal to zero, and take a diffusion coefficient Γ that is discontinuous across a curve in $\Omega = (0,1) \times (0,1)$

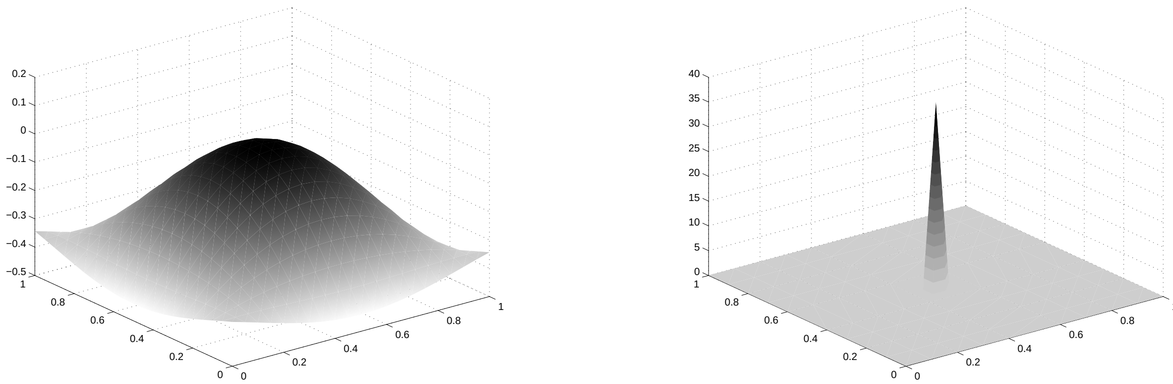

Figure 4: Source term (left figure) and exact solution (right figure) of the two-dimensional interface problem.

and has a small value in part of the domain, viz.

$$\Gamma(x,y) := \begin{cases} \delta, & \text{for } (x,y) \in U_\varepsilon, \\ 1, & \text{for } (x,y) \in \Omega \setminus U_\varepsilon, \end{cases}$$

where $0 < \delta \ll 1$, $U_\varepsilon := (1/2-\varepsilon, 1/2+\varepsilon) \times (1/2-\varepsilon, 1/2+\varepsilon)$, $0 < \varepsilon < 1/2$. The boundary conditions ψ and right hand side s are chosen such that the solution to the continuous problem is known and has a high activity region in U_ε. If we define the auxiliary function $a : I\!R \to I\!R$ by

$$a(x) := \exp\left(-(x-1/2)^2\right) - \exp(-\varepsilon^2),$$

and set

$$\begin{aligned} \psi(x,y) &:= a(x)\,a(y), && (x,y) \in \partial\Omega, \\ s(x,y) &:= -a''(x)\,a(y) - a(x)\,a''(y), && (x,y) \in \Omega, \end{aligned}$$

we have the following expression for the solution φ of the continuous problem:

$$\varphi(x,y) = \begin{cases} \delta^{-1}\,a(x)\,a(y), & \text{for } (x,y) \in U_\varepsilon, \\ a(x)\,a(y), & \text{for } (x,y) \in \Omega \setminus U_\varepsilon. \end{cases}$$

Note that ψ and s depend on ε but not on δ. In the experiment below, we take $\delta = 10^{-8}$, $\varepsilon = 2/81$. The source term s and the exact solution φ with these values of δ and ε are shown in Figure 4.
Because of the different resolutions needed to represent φ in U_ε and $\Omega \setminus U_\varepsilon$, we will use the LDC method with the finite volume adapted correction term as described in Section 3.2 to discretize the boundary value problem for φ on a *composite* grid. We take $\Omega_l := (1/2 - 1/27, 1/2+1/27) \times (1/2-1/27, 1/2+1/27)$. For the global coarse grid, meshsizes $H = 1/3^3$, $H = 1/3^4$, and $H = 1/3^5$ have been used; the refinement factor σ has been chosen equal to $\sigma = 3$, $\sigma = 3^2$, and $\sigma = 3^3$. In this model problem, the location of the physical interface (∂U_ε) is such that for $H = 1/3^k$, $k \geq 3$, and $\sigma = 3^m$, $m \geq 1$, this interface is on grid lines in Ω_l^h. Therefore, a simple central difference flux approximation scheme, as in Example 1, can be

	$H = 1/3^3$		$H = 1/3^4$		$H = 1/3^5$	
	Unknowns	Error	Unknowns	Error	Unknowns	Error
$h = 1/3^3$	729	$1.7 \cdot 10^{+0}$				
$h = 1/3^4$	778	$1.1 \cdot 10^{-4}$	6561	$7.4 \cdot 10^{-5}$		
$h = 1/3^5$	1090	$1.6 \cdot 10^{-5}$	6922	$8.3 \cdot 10^{-6}$	59049	$8.3 \cdot 10^{-6}$
$h = 1/3^6$	3754	$1.2 \cdot 10^{-5}$	9586	$1.5 \cdot 10^{-6}$	62074	$9.3 \cdot 10^{-7}$

Table 1: Numerical results for the two-dimensional interface problem computed using the LDC algorithm with finite volume adapted correction term on a composite grid. The global coarse grid has meshsize H; the local fine grid has meshsize h.

used (see [18] for a more detailed discussion of this topic). In a setting where this favorable interface-grid alignment does not hold, other, more advanced, finite volume discretization schemes should be used. The LDC method, however, remains the same.

Since the main topic of this paper is to study the performance of the LDC (outer) iteration, the linear systems arising in the LDC algorithm have been solved to high accuracy using CG iteration with incomplete Cholesky factorization as a preconditioner. The properties shown below still hold, however, if we use low, but "reasonable", accuracy in the inner iterations.

The numerical results of the LDC method are presented in Table 1. Listed are the number of unknowns in the computation and the discretization error in the scaled Euclidean norm $\left\| \varphi|_{\Omega^H} - \boldsymbol{\varphi}_*^H \right\|_2 / N$, where N is such that N^2 is the number of grid points in Ω^H. Note that diagonal elements in the table correspond to uniform grids. From Table 1, we conclude that the LDC algorithm can reduce the discretization error on the global coarse grid (meshsize H) to an error that is of the same order of magnitude as the error on a global uniform grid with meshsize h, using considerably less grid points than a computation on a global uniform grid with meshsize h would require. This is, e.g., illustrated by the computation on the composite grid with meshsizes $H = 1/3^4$, $h = 1/3^5$, which uses only 6922 grid points to find an approximation with the same error as a computation on a uniform grid with meshsize $H = 1/3^5$, which involves 59049 unknowns. Note that even the error in the result on the composite grid with $H = 1/3^3$, $h = 1/3^5$, which has only 1090 grid points, is already of the same order of magnitude.

Finally, we remark that the uniform grid with meshsize $H = 1/3^3$ completely misses the high activity region U_ε, causing a very large discretization error. This error is reduced by a factor of order 10^4 by refining the high activity zone with a factor σ of only 3 (introducing just 49 new grid points).

The excellent rate of convergence of the LDC method is illustrated by the fact that the results in Table 1 are already found after just one LDC correction step. In other words, a table listing the discretization error $\left\| \varphi|_{\Omega^H} - \boldsymbol{\varphi}_1^H \right\|_2 / N$, would be the same as Table 1.

If in this experiment, we use the standard correction term as in [11] instead of the new correction term $\mathbf{S}^H(\boldsymbol{\varphi}^{H,h})$ as in (22), we obtain similar results. This is not surprising, since the conservation property is crucial across the physical interface ∂U_ε, but of minor importance across the artificial interface Γ. Hence, using a finite volume discretization for the local fine grid problem is of major importance, but using the new correction term, which yields conservation across Γ, is of minor importance.

4.2 A one-dimensional time dependent convection-diffusion problem

In this section, we treat a very simple one-dimensional problem, in which global conservation is crucial. For this problem, the results of the classical LDC algorithm as in $[6, 7, 11]$ are very poor, whereas the finite volume adapted algorithm yields satisfactory results.
We consider a time dependent convection-diffusion problem, which is a model for the behavior of water held inside a basin by two levies. We choose the following values for the parameters in the problem. The diffusion coefficient Γ equals one in $\Omega = (0, 1)$. The mass flux is time dependent: $v(x, t) := 10 + 25 \sin(20\, t)$, $x \in \bar{\Omega}$, $t \geq 0$. There is no production or consumption in the domain, hence $s(x) := 0$, $x \in \Omega$. This leads to the following partial differential equation for φ in Ω:

$$\frac{\partial \varphi}{\partial t} + \frac{\partial}{\partial x}(f_\varphi) = 0, \qquad f_\varphi := v\varphi - \frac{\partial \varphi}{\partial x},$$

which expresses the tendency of the water level φ to follow the wind v, and to level out. We choose flux boundary conditions, viz. $f_\varphi(0, t) = 0$, $f_\varphi(1, t) = 0$, which model the two levies that prevent the water from flowing in or out of the basin. The initial condition is $\varphi(x, 0) = 1$. Integration of the partial differential equation over Ω yields the global conservation law

$$\frac{\partial}{\partial t} \int_0^1 \varphi(x, t)\, dx = 0. \tag{35}$$

We first applied the Euler Backward method for the time discretization. In each Euler step, a continuous two-point boundary value problem has to be solved. Because of boundary layer effects, the water level varies most in the outer parts of the spatial domain, i.e., in $(0, \delta)$ and in $(1 - \delta, 1)$. For this reason we will use a composite grid for space discretization. The composite grid used consists of a global coarse grid with meshsize $H = 1/20$ in Ω and two local fine grids, both with meshsize $h = 1/100$, in $\Omega_{l,1} := (0, 1/8)$ and in $\Omega_{l,2} := (7/8, 1)$. We present results for both the LDC method with the standard choice for the correction term and the LDC method with the finite volume adapted correction term. The results are shown in Figure 5.
Clearly, the LDC method with the standard choice for the correction term leads to an unrealistic and decreasing water level through "numerical evaporation". The LDC method with the finite volume adapted correction term satisfies a discrete equivalent of the global conservation law (35), and preserves the water level.

References

[1] Arney, D.C. and J.E. Flaherty, An adaptive local mesh refinement method for time dependent partial differential equations, *Appl. Numer. Math.*, 5 (1989), pp. 257–274.

[2] Berger, M.J. and P. Colella, Local adaptive mesh refinement for shock hydrodynamics, *J. Comput. Phys.*, 82 (1989), pp. 64–84.

[3] Ewing, R.E., Adaptive grid refinements for transient flow problems, in: *Adaptive Methods for Partial Differential Equations*, J.E. Flaherty, P.J. Paslow, M.S. Shephard and J.D. Vasilakis (eds.), pp. 194–205, SIAM, Philadelphia (1989).

[4] Ewing, R.E., R.D. Lazarov and P.S. Vassilevski, Local refinement techniques for elliptic problems on cell-centered grids. I: error analysis, *Math. Comp.*, 56 (1991), pp. 437–461.

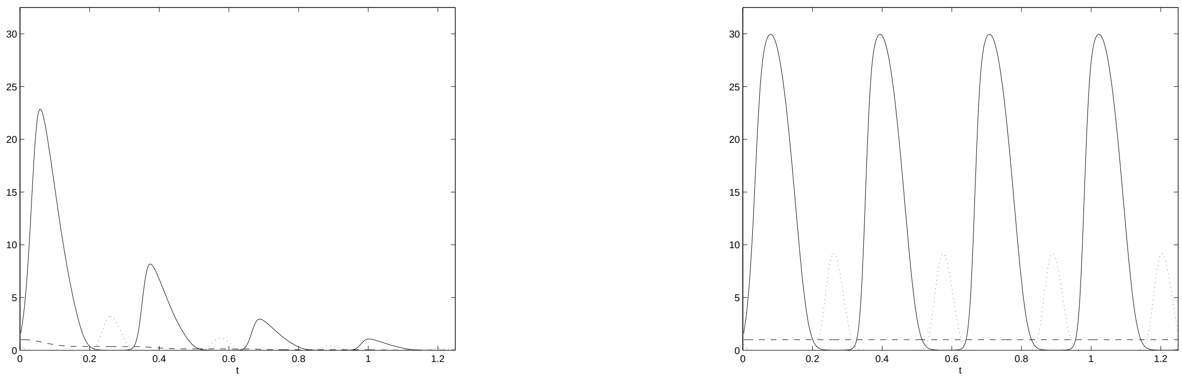

Figure 5: Numerical results computed using the LDC algorithm with the standard choice for the correction term (left figure) and with the finite volume adapted correction term (right figure). The dotted, solid and dashed curves indicate the approximations of $\varphi(0,t)$, $\varphi(1,t)$, and $\int_0^1 \varphi(x,t)\,dx$, respectively.

[5] Ferket, P.J.J., *Solving Boundary Value Problems on Composite Grids with an Application to Combustion*, Ph.D. Thesis, Eindhoven University of Technology, Eindhoven (1996).

[6] Ferket, P.J.J. and A. Reusken, Further analysis of the Local Defect Correction Method, *Computing*, 56 (1996), pp. 117–139.

[7] Ferket, P.J.J. and A. Reusken, A finite difference discretization method on composite grids, *Computing*, 56 (1996), pp. 343–369.

[8] Flaherty, J.E., P.K. Moore and C. Ozturan, Adaptive overlapping grid methods for parabolic systems, in: *Adaptive Methods for Partial Differential Equations*, J.E. Flaherty, P.J. Paslow, M.S. Shephard and J.D. Vasilakis (eds.), pp. 176–193, SIAM, Philadelphia (1989).

[9] Gropp, W.D., Local uniform mesh refinement with moving grids, *SIAM J. Sci. Stat. Comput.*, 8 (1987), pp. 292–304.

[10] Gropp, W.D. and D.E. Keyes, Domain decomposition with local mesh refinement, *SIAM J. Sci. Comput.*, 13 (1992), pp. 967–993.

[11] Hackbusch, W., Local defect correction method and domain decomposition techniques, *Computing*, Suppl. 5 (1984), pp. 89–113.

[12] Heinrich, B., *Finite Difference Methods on Irregular Networks*, International Series of Numerical Mathematics, Vol. 82, Birkhäuser, Basel (1987).

[13] Hirsch, C., *Numerical Computation of Internal and External Flows, Vol. I: Fundamentals of Numerical Discretization*, Wiley, Chichester (1988).

[14] Kröner, D., *Numerical Schemes for Conservation Laws*, Wiley, Teubner, Chichester (1997).

[15] McCormick, S.F., *Multilevel Adaptive Methods for Partial Differential Equations*, Frontiers in Applied Mathematics, Vol. 6, SIAM, Philadelphia (1989).

[16] McCormick, S.F. and J. Thomas, The fast adaptive composite grid (FAC) method for elliptic equations, *Math. Comp.*, 46 (1986), pp. 439–456.

[17] Thomas, J.W., R. Schweitzer, M. Heroux, S. McCormick and A.M. Thomas, Application of the fast adaptive composite grid method to computational fluid dynamics, in *Numerical Methods in Laminar and Turbulent Flow*, (1987), pp. 1071–1082.

[18] Wesseling, P., *An Introduction to Multigrid Methods*, Wiley, Chichester (1992).

[19] Wesseling, P., Large scale modeling in computational dynamics, in: *Algorithms and Parallel VLSI Architectures, Volume A: Tutorials*, E.F. Deprettere and A.J. van der Veen (eds.), pp. 277–306, Elsevier (1991).

M.J.H. Anthonissen, B. van 't Hof
Department of Mathematics and Computing Science
Eindhoven University of Technology
P.O. Box 513, 5600 MB Eindhoven, The Netherlands
e-mail: martijna@@win.tue.nl, bas@@win.tue.nl

A.A. Reusken
Institut für Geometrie und Praktische Mathematik
RWTH Aachen
Templergraben 55, D-52056 Aachen, Germany
e-mail: reusken@@igpm.rwth-aachen.de